LETTER

doi:10.1038/nature09396

Recent decline in the global land evapotranspiration trend due to limited moisture supply

Martin Jung[1], Markus Reichstein[1], Philippe Ciais[2], Sonia I. Seneviratne[3], Justin Sheffield[4], Michael L. Goulden[5], Gordon Bonan[6], Alessandro Cescatti[7], Jiquan Chen[8], Richard de Jeu[9], A. Johannes Dolman[9], Werner Eugster[10], Dieter Gerten[11], Damiano Gianelle[12], Nadine Gobron[13], Jens Heinke[11], John Kimball[14], Beverly E. Law[15], Leonardo Montagnani[16], Qiaozhen Mu[17], Brigitte Mueller[3], Keith Oleson[6], Dario Papale[18], Andrew D. Richardson[19], Olivier Roupsard[20], Steve Running[17], Enrico Tomelleri[1], Nicolas Viovy[2], Ulrich Weber[1], Christopher Williams[21], Eric Wood[4], Sönke Zaehle[1] & Ke Zhang[14]

More than half of the solar energy absorbed by land surfaces is currently used to evaporate water[1]. Climate change is expected to intensify the hydrological cycle[2] and to alter evapotranspiration, with implications for ecosystem services and feedback to regional and global climate. Evapotranspiration changes may already be under way, but direct observational constraints are lacking at the global scale. Until such evidence is available, changes in the water cycle on land—a key diagnostic criterion of the effects of climate change and variability—remain uncertain. Here we provide a data-driven estimate of global land evapotranspiration from 1982 to 2008, compiled using a global monitoring network[3], meteorological and remote-sensing observations, and a machine-learning algorithm[4]. In addition, we have assessed evapotranspiration variations over the same time period using an ensemble of process-based land-surface models. Our results suggest that global annual evapotranspiration increased on average by 7.1 ± 1.0 millimetres per year per decade from 1982 to 1997. After that, coincident with the last major El Niño event in 1998, the global evapotranspiration increase seems to have ceased until 2008. This change was driven primarily by moisture limitation in the Southern Hemisphere, particularly Africa and Australia. In these regions, microwave satellite observations indicate that soil moisture decreased from 1998 to 2008. Hence, increasing soil-moisture limitations on evapotranspiration largely explain the recent decline of the global land-evapotranspiration trend. Whether the changing behaviour of evapotranspiration is representative of natural climate variability or reflects a more permanent reorganization of the land water cycle is a key question for earth system science.

Land evapotranspiration (ET) is a central process in the climate system and a nexus of the water, energy and carbon cycles. Global land ET returns about 60% of annual land precipitation to the atmosphere[5]. Terrestrial ET can affect precipitation[6], and the associated latent heat flux helps to control surface temperatures, with important implications for regional climate characteristics such as the intensity and duration of heat waves[7,8].

Acceleration or intensification of the hydrological cycle with global warming is a long-standing paradigm in climate research[2], but direct observational evidence of a positive trend in global ET is still lacking. A global network (FLUXNET) of continuous *in situ* measurements of land–atmosphere exchanges, including of water vapour, has been established over the last decade[3], and these data can be used to estimate global ET dynamics. We have designed an approach to assessing the temporal behaviour and global spatial distribution of ET over the past 27 years. It integrates point-wise ET measurements at the FLUXNET observing sites with geospatial information from satellite remote sensing and surface meteorological data in a machine-learning algorithm (the model tree ensemble or MTE; ref 4). The approach is data-driven and thus largely independent of theoretical-model assumptions.

We estimate a mean annual global land-surface ET value from 1982 to 2008 of $65 \pm 3 \times 10^3$ km^3 per year, with the spatial distribution shown in Fig. 1a. This estimate is consistent with the value reported in ref. 5 (65.5×10^3 km^3 per year), and falls within the model range (58×10^3–85×10^3 km^3 per year) estimated by the Global Soil Wetness Project 2 (GSWP-2; ref. 9). The validity of our data-driven ET product is supported by internal cross-validation at FLUXNET sites (Fig. 1b), corroboration against independent ET estimates from 112 catchment water balances (Fig. 1c), and the simulations of 16 land-surface models participating in GSWP-2 (Fig. 1d and Supplementary Methods Section 6; ref. 9).

Our global land-ET estimate, derived from FLUXNET, remote sensing and meteorological observations, suggests that the rate of land ET increased from the early 1980s to the late 1990s with a linear trend of 7.1 ± 1 mm per year per decade for 1982–1997 ($P < 0.01$ according to the Mann–Kendall test). The positive ET trend shown in Fig. 2 is consistent with the expected 'acceleration' of the hydrological cycle caused by an increased evaporative demand associated with rising radiative forcing[10] and temperatures. Indeed, interannual variability in temperature correlates well with ET variability from 1982 to 1997 (Pearson's correlation coefficient 0.84, $P < 0.01$). This trend of rising land ET disappears after the last big El Niño event in 1998, and the subsequent decline of the global terrestrial ET trend is consistent with estimates from nine process-oriented ET land-surface models (see Supplementary Table 5) driven by meteorological fields and vegetation states (Fig. 2 and Supplementary Discussion Section 2). The trend of the median global land-ET anomalies derived from these models becomes negative during 1998–2008 (−7.9 mm per year per decade, $P < 0.05$). We are cautious regarding the robustness of this recent ET

[1]Max Planck Institute for Biogeochemistry, 07745 Jena, Germany. [2]Laboratoire des Sciences du Climat et de l'Environment (LSCE), Joint Unit of Commissariat à l'énergie atomique et aux énergies alternatives (CEA), Centre national de la recherche scientifique (CNRS) and l'Université de Versailles Saint-Quentin (UVSQ), F-91191 Gif-sur-Yvette, France. [3]Institute for Atmospheric and Climate Science, ETH Zurich, CH-8092 Zurich, Switzerland. [4]Department of Civil and Environmental Engineering, Princeton University, New Jersey 08544, USA. [5]Department of Earth System Science, University of California, Irvine, California 92697-3100, USA. [6]National Center for Atmospheric Research, Boulder, Colorado 80307-3000, USA. [7]European Commission — Directorate General Joint Research Centre, Institute for Environment and Sustainability, Climate Change Unit, I-21027 Ispra (VA), Italy. [8]Department of Environmental Sciences, University of Toledo, Toledo, Ohio 43606-3390, USA. [9]Department of Hydrology and Geo-environmental Sciences, Faculty of Earth and Life Scienes, Vrije Universiteit, 1081 HV Amsterdam, Netherlands. [10]Institute of Plant Sciences, ETH Zurich, CH-8092 Zurich, Switzerland. [11]Potsdam Institute for Climate Impact Research, Research Domain of Climate Impacts and Vulnerabilities, 14473 Potsdam, Germany. [12]Istituto Agrario San Michele all'Adige, Research and Innovation Centre, Fondazione Edmund Mach, Environment and Natural Resources Area, Trento, Italy. [13]European Commission – DG Joint Research Centre, Institute for Environment and Sustainability, Global Environmental Monitoring Unit, I-21027 Ispra (VA), Italy. [14]Flathead Lake Biological Station, Division of Biological Sciences, University of Montana, Polson, Montana 59860 -6815, USA. [15]Department of Forest Ecosystems and Society, Oregon State University, Corvallis, Oregon 97331, USA. [16]Forest Services and Agency for the Environment, Autonomous Province of Bolzano, 39100 Bolzano, Italy. [17]Numerical Terradynamic Simulations Group, College of Forestry & Conservation, University of Montana, Missoula, Montana 59812, USA. [18]Department of Forest Environment and Resources, University of Tuscia, 01100 Viterbo, Italy. [19]Department of Organismic and Evolutionary Biology, Harvard University, Cambridge, Massachusetts 02138, USA. [20]Cirad-Persyst, UPR 80, Fonctionnement et Pilotage des Ecosystèmes de Plantations, 34060 Montpellier, France. [21]Graduate School of Geography, Clark University, Worcester, Massachusetts 01610-1477, USA.

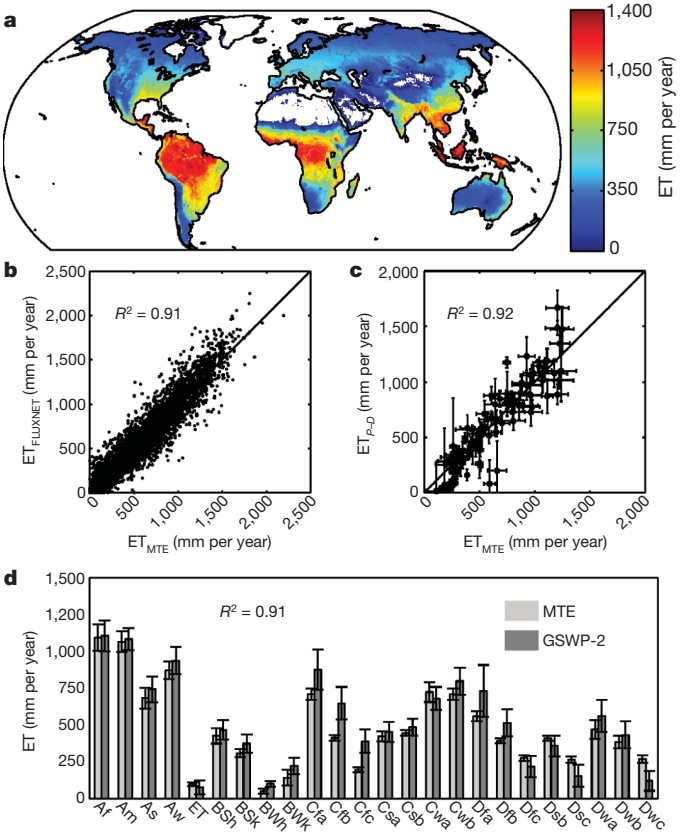

Figure 1 | Validation of global land ET product from MTE. **a**, Map of mean annual ET (1982–2008) in mm per year from MTE. **b**, Performance of MTE in predicting monthly ET at FLUXNET sites ($n = 4{,}678$), based on internal ten-fold cross-validation (units converted to millimetres per year for consistency). R^2, coefficient of determination. **c**, Comparison of mean annual MTE ET against mean annual ET from catchment water balance calculated as precipitation (P) minus discharge (D) ($n = 112$). **d**, Comparison of annual MTE ET (1986–1995) stratified by bioclimatic zones (n = 24) against the median GSWP-2 model ensemble. All error bars are one s.d. See Supplementary Methods Section 6 for details. Af, equatorial, fully humid; Am, equatorial, monsoonal; As, equatorial, summer dry; Aw, equatorial, winter dry; BWk, cold arid desert; BWh, hot arid desert; BSk, cold arid steppe; BSh, hot arid steppe; Cfa, humid, warm temperate, hot summer; Cfb, humid, warm temperate, warm summer; Cfc, humid, warm temperate, cool summer; Csa, summer dry, warm temperate, warm summer; Csb, summer dry, warm temperate, warm summer; Cwa, winter dry, warm temperate, hot summer; Cwb, winter dry, warm temperate, warm summer; Dfa, snow, humid, hot summer; Dfb, snow, humid, warm summer; Dfc, snow, humid, cool summer; Dsb, snow, summer dry, warm summer; Dsc, snow, summer dry, cool summer; Dwa, snow, winter dry, hot summer; Dwb, snow, winter dry, warm summer; Dwc, snow, winter dry, cool summer; ET, polar tundra.

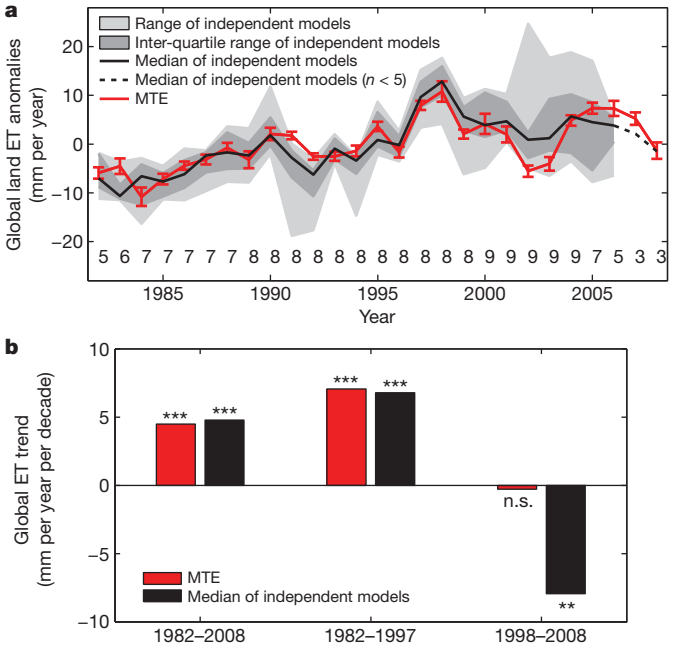

Figure 2 | Global land-ET variability according to MTE and independent models. **a**, Annual global land ET anomalies based on MTE and an ensemble of up to nine independent process-oriented models. Error bars indicate one s.d. within the MTE. Numbers at the bottom show the number of models available each year. **b**, Trends in ET based on MTE estimates and based on the median of the independent models for three different time periods. ***, significance of the trends at the 99% confidence interval; **, significance of the trends at the 95% confidence interval; n.s., not significant.

slowdown, given that the ensemble median is based on only relatively few models towards the end of the period.

Distinguishing land-ET response due to atmospheric demand from that due to terrestrial moisture-supply limitation is a classic ecohydrological problem[11,12]. ET responds to changing atmospheric demand, for example to changing radiation, or to changing vapour-pressure deficit, which is often associated with temperature, if there is sufficient moisture supply. In contrast, if the soils are too dry, ET becomes restricted by soil moisture. We analysed the spatial pattern of ET-trend changes and found that the largest regional contributions to the declining trend in global ET since 1998 originate from the Southern Hemisphere in Africa and Australia (Fig. 3). The largest trend declines seem to have occurred in regions in which ET is limited by moisture (see Supplementary Methods Section 7). In these regions, lower ET would in turn be expected to feed back to the atmosphere and increase atmospheric dryness. A recent decrease in atmospheric relative humidity detected over Australia[13] could be caused by declining ET on the Australian continent.

We wondered whether a soil moisture shortage could be the reason for the decline of the ET trend since 1998. Satellite microwave remote sensing provides consistent large-scale information on soil moisture, although these sensors are only sensitive to the moisture of the upper few centimetres of the soil and the associated uncertainties are large for regions of dense vegetation[14]. The Tropical Rainfall Measuring Mission's (TRMM) microwave imager currently yields the longest high-quality record of surface soil moisture since 1998 (ref. 15). The TRMM imaging area is confined to latitudes between 38° S and 38° N, but covers the regions in which the largest ET-trend changes occurred. We found strong coherence between 1998–2008 ET trends derived from FLUXNET data using the MTE approach, and trends in the independent TRMM satellite-observed surface soil moisture in those regions in which moisture supply is expected to control ET (Fig. 4a, b). The Southern Hemisphere pattern of decreasing ET is matched by a soil-moisture decrease over large parts of Australia, East Africa and South America. The coherence between temporal ET and soil-moisture variability remains even when they are averaged over the whole TRMM domain (Fig. 4c). We can rule out the hypothesis that ET changes are caused by changes in atmospheric demand in these regions. Trends in atmospheric demand assessed with potential ET are in the opposite direction to trends in actual ET (Supplementary Figs 5 and 6), except in China and southern India, where potential ET and ET both exhibit positive trends. In these regions ET and soil-moisture trends are opposed, probably because ET remains primarily demand-limited (see Supplementary Fig. 2). Hence, increasing ET due to increasing atmospheric demand (see Supplementary Fig. 5) depletes soil moisture, but not to the extent that it would in turn limit ET.

The strong spatial consistency of the patterns in the independently estimated ET and soil-moisture trends suggests that decreasing soil moisture supply in the Southern Hemisphere is the main mechanism contributing to the cessation of the rising ET trend after 1998. Other mechanisms that could be responsible for a stabilization of global land

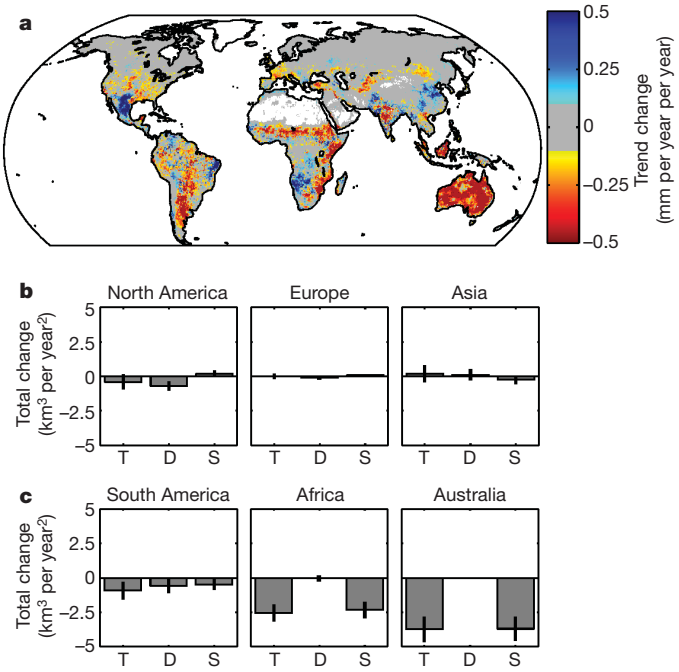

Figure 3 | ET trend changes. **a**, Map of the change in ET trend between 1982–1997 and 1998–2008 in millimetres per year per year. Small trend changes of ±0.1 mm per year per year are shown in grey to enhance clarity. Total continental contributions of North America, Europe and Asia (**b**) and South America, Africa and Australia (**c**) in cubic kilometres per year per year. T, total area; D, demand-limited area; S, supply-limited area (see Supplementary Fig. 4). Error bars refer to one s.d. and are derived from the individual members of the MTE.

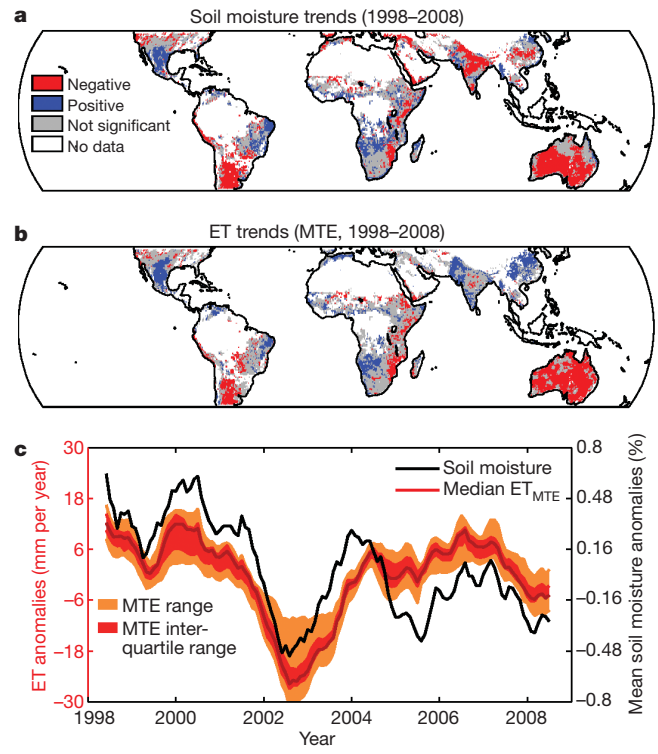

Figure 4 | Soil-moisture and ET trends. Significant ($P < 0.1$) soil-moisture trends derived from TRMM (**a**), significant ($P < 0.1$) ET trends from MTE (**b**) and mean ET and soil-moisture anomalies (seasonal cycle subtracted and filtered with an 11-month running mean) of all valid pixels of the TRMM domain (**c**). For consistency and improved comparability, regions without data in either MTE (non-vegetated areas) or TRMM soil-moisture data (very dense vegetation) are blanked in the trend maps of **a** and **b**.

ET seem to be less important; they include stomata closure caused by increasing CO_2 concentrations[16], land-use change[17], or decreasing wind speed[18]. More-detailed analyses[17,19,20] did not find a measurable effect on the global land hydrological cycle caused by increased efficiency of water-use in ecosystems under rising atmospheric CO_2 concentrations, as was suggested in ref. 16. Land-use change is likely to have an important role regionally, but is apparently too geographically confined to govern the recent global ET trends. Decreasing surface wind speeds have also been put forward as a possible cause for regional decline of potential evapotranspiration[18], but if lower surface wind speeds were responsible for the recent levelling-off of actual evapotranspiration, we would not see the largest changes in supply-limited regions.

In conclusion, we provide a data-driven, spatially explicit estimate of global terrestrial evapotranspiration over the past 27 years by combining *in situ* measurements, meteorology and remote-sensing information. We infer a rising trend in land-surface ET between 1982 and 1997. This trend seems to have declined since then, probably because of soil-moisture limitation. Owing to the relatively short time period we cannot precisely date a 'switch' in behaviour, but our analysis suggests that the late 1990s mark a transition period in which the global land-ET trend decreases. It is hard to evaluate whether this is part of a natural climate oscillation, or a climate-change signal in which land evapotranspiration becomes more and more supply-limited in the long term. The latter would imply that there is a limit to energy- and temperature-driven acceleration of the terrestrial hydrological cycle, and that it may have been reached. The consequences would be decreasing terrestrial productivity and a reduced terrestrial carbon sink, preferential partitioning of energy fluxes at the land surface into sensible, rather than latent, heat flux and thus accelerated land-surface warming, and intensified regional land–atmosphere feedback[6].

METHODS SUMMARY

We processed half-hourly eddy covariance data from 253 globally distributed flux towers[3] using standardized gap-filling and quality-control algorithms[21,22] and a correction for incomplete energy balance closure[23]. This yielded a global data set composed of monthly estimates of local ET and meteorological records from each tower (a total of 4,678 site-months within the period 1997–2006), along with satellite observations of the fraction of photosynthetically active radiation absorbed by the canopy (FAPAR) at 2-km resolution from the sea-viewing wide field-of-view sensor (SeaWiFS; ref. 24), and site-level information on vegetation type and local climate (Supplementary Data Section 1). We used this global data set to train the MTE to create maps of gridded monthly ET at 0.5° resolution covering the whole period 1982–2008. Owing to a lack of measurements in cold and dry deserts, we do not account for non-vegetated areas; this probably results in a small underestimation of the global total ET value. We used an ensemble of 25 model trees to define a median best-estimate and uncertainty based on the spread of the estimates among the individual trees in the ensemble[4]. We used a harmonized FAPAR product from three sensors (AVHRR[25], SeaWiFS[24], MERIS[26]), a remote-sensing-based global land-use map[27], and observation-based products of climate variables[28,29] as forcing data. We estimated significance levels of trends on the basis of Mann–Kendall tests. We estimated the slopes of the trends as described in ref. 30.

Received 7 October 2009; accepted 6 August 2010.

Published online 10 October; corrected 21 October 2010 (see full-text HTML version for details).

1. Trenberth, K. E., Fasullo, J. T. & Kiehl, J. Earth's global energy budget. *Bull. Am. Meteorol. Soc.* **90,** 311–323 (2009).
2. Huntington, T. G. Evidence for intensification of the global water cycle: review and synthesis. *J. Hydrol.* **319,** 83–95 (2006).
3. Baldocchi, D. 'Breathing' of the terrestrial biosphere: lessons learned from a global network of carbon dioxide flux measurement systems. *Aust. J. Bot.* **56,** 1–26 (2008).
4. Jung, M., Reichstein, M. & Bondeau, A. Towards global empirical upscaling of FLUXNET eddy covariance observations: validation of a model tree ensemble approach using a biosphere model. *Biogeosciences* **6,** 2001–2013 (2009).
5. Oki, T. & Kanae, S. Global hydrological cycles and world water resources. *Science* **313,** 1068–1072 (2006).

6. Koster, R. D. *et al.* Regions of strong coupling between soil moisture and precipitation. *Science* **305,** 1138–1140 (2004).
7. Seneviratne, S. I., Lüthi, D., Litschi, M. & Schär, C. Land–atmosphere coupling and climate change in Europe. *Nature* **443,** 205–209 (2006).
8. Vautard, R. *et al.* Summertime European heat and drought waves induced by wintertime Mediterranean rainfall deficit. *Geophys. Res. Lett.* L07711 (2007).
9. Dirmeyer, P. A. *et al.* GSWP-2: Multimodel analysis and implications for our perception of the land surface. *Bull. Am. Meteorol. Soc.* **87,** 1381–1397 (2006).
10. Wild, M., Grieser, J. & Schär, C. Combined surface solar brightening and increasing greenhouse effect support recent intensification of the global land-based hydrological cycle. *Geophys. Res. Lett.* **35,** L17706 (2008).
11. Budyko, M. I. *Climate and Life* (Academic, 1974).
12. Seneviratne, S. I. *et al.* Investigating soil moisture–climate interactions in a changing climate: a review. *Earth Sci. Rev.* **99,** 99–174 (2010).
13. Simmons, A., Willett, K. M., Jones, P. D., Thorne, P. W. & Dee, D. Low-frequency variations in surface atmospheric humidity, temperature, and precipitation: inferences from reanalyses and monthly gridded observational data sets. *J. Geophys. Res.* **115,** D01110 (2010).
14. Scipal, K., Holmes, T. R. H., de Jeu, R. A. M., Naeimi, V. & Wagner, W. W. A possible solution for the problem of estimating the error structure of global soil moisture datasets. *Geophys. Res. Lett.* **35,** L24403 (2008).
15. Owe, M., De Jeu, R. A. M. & Holmes, T. R. H. Multisensor historical climatology of satellite-derived global land surface moisture. *J. Geophys. Res.* **113,** F01002 (2007).
16. Gedney, N. *et al.* Detection of a direct carbon dioxide effect in continental river runoff records. *Nature* **439,** 835–838 (2006).
17. Piao, S. *et al.* Changes in climate and land use have a larger direct impact than rising CO_2 on global river runoff trends. *Proc. Natl Acad. Sci. USA* **104,** 15242–15247 (2007).
18. Roderick, M. L., Rotstayn, L. D., Farquhar, G. & Hobbins, M. T. On the attribution of changing pan evaporation. *Geophys. Res. Lett.* **34,** L17403 (2007).
19. Gerten, D., Rost, S., von Bloh, W. & Lucht, W. Causes of change in 20th century global river discharge. *Geophys. Res. Lett.* **35,** L20405 (2008).
20. Milliman, J. D., Farnsworth, K. L., Jones, P. D., Xu, K. H. & Smith, L. C. Climatic and anthropogenic factors affecting river discharge to the global ocean, 1951–2000. *Global Planet. Change* **62,** 187–194 (2008).
21. Moffat, A. M. *et al.* Comprehensive comparison of gap-filling techniques for eddy covariance net carbon fluxes. *Agric. For. Meteorol.* **147,** 209–232 (2007).
22. Papale, D. *et al.* Towards a standardized processing of net ecosystem exchange measured with eddy covariance technique: algorithms and uncertainty estimation. *Biogeosciences* **3,** 571–583 (2006).
23. Twine, T. E. *et al.* Correcting eddy-covariance flux underestimates over a grassland. *Agric. For. Meteorol.* **103,** 279–300 (2000).
24. Gobron, N. *et al.* Evaluation of fraction of absorbed photosynthetically active radiation products for different canopy radiation transfer regimes: methodology and results using JRC products derived from SeaWiFS against ground-based estimations. *J. Geophys. Res.* **111,** D13110 (2006).
25. Tucker, C. *et al.* An extended AVHRR 8-km NDVI data set compatible with MODIS and SPOT vegetation NDVI data. *Int. J. Remote Sens.* **26,** 4485–4498 (2005).
26. Gobron, N. *et al.* Uncertainty estimates for the FAPAR operational products derived from MERIS — impact of top-of-atmosphere radiance uncertainties and validation with field data. *Remote Sens. Environ.* **112,** 1871–1883 (2008).
27. Jung, M., Henkel, K., Herold, M. & Churkina, G. Exploiting synergies of global land cover products for carbon cycle modeling. *Remote Sens. Environ.* **101,** 534–553 (2006).
28. Österle, H., Gerstengarbe, F.-W. & Werner, P. C. Homogenisierung und Aktualisierung des Klimadatensdatzes der Climate Research Unit of East Anglia, Norwich. *Terra Nostra* **6,** 326–329 (2003).
29. Schneider, U., Fuchs, T., Meyer-Christoffer, A. & Rudolf, B. *Global Precipitation Analysis Products of the GPCC.* (Global Precipitation Climatology Centre, 2008).
30. Sen, P. K. Estimates of the regression coefficient based on Kendall's tau. *J. Am. Stat. Assoc.* **63,** 1379–1389 (1968).

Supplementary Information is linked to the online version of the paper at www.nature.com/nature.

Acknowledgements This work used eddy covariance data acquired by the FLUXNET community and in particular by the following networks: AmeriFlux (US Department of Energy, Biological and Environmental Research, Terrestrial Carbon Program; DE-FG02-04ER63917 and DE-FG02-04ER63911), AfriFlux, AsiaFlux, CarboAfrica, CarboEuropeIP, CarboItaly, CarboMont, ChinaFlux, Fluxnet-Canada (supported by the Canadian Foundation for Climate and Atmospheric Sciences, the Natural Sciences and Engineering Research Council of Canada, BIOCAP, Environment Canada and Natural Resources Canada), GreenGrass, KoFlux, the Largescale Biosphere–Atmosphere Experiment in Amazonia, the Nordic Centre for Studies of Ecosystem Carbon Exchange, OzFlux, the Terrestrial Carbon Observatory System Siberia and US–China Carbon Consortium. We acknowledge the support to the eddy covariance data harmonization provided by CarboEuropeIP; the Food and Agriculture Organization of the United Nations' Global Terrestrial Observing System Terrestrial Carbon Observations; the Integrated Land Ecosystem–Atmosphere Processes Study, a core project of the International Geosphere–Biosphere Programme; the Max Planck Institute for Biogeochemistry; the National Science Foundation; the University of Tuscia; Université Laval; Environment Canada; and the US Department of Energy. We acknowledge database development and technical support from Berkeley Water Center, Lawrence Berkeley National Laboratory, Microsoft Research eScience, Oak Ridge National Laboratory, University of California, Berkeley and University of Virginia. We thank the members of FLUXNET (http://www.fluxdata.org/DataInfo) for their help with the data on this work. TRMM soil moisture retrievals and analysis were supported by the European Union (FP6) funded integrated project called WATCH (contract number 036946) that supported A.J.D. and R.d.J. M.J. and M.R. were supported by the European Union (FP7) integrated project COMBINE (number 226520) and a grant from the Max-Planck Society establishing the MPRG Biogeochemical Model-Data Integration. C.W. was supported by the US National Science Foundation under grant ATM-0910766. D.P. acknowledges the support of the Euro–Mediterranean Centre for Climate Change. We acknowledge institutions and projects for free access to relevant data: the Global Runoff Data Centre, the Global Soil Wetness Project 2, the Global Precipitation Climatology Centre, the Global Precipitation Climatology Project, the Global Historical Climatology Network, the Potsdam Institute for Climate Impact Research, the University of East Anglia, the National Oceanic and Atmospheric Administration Earth System Research Laboratory and the European Centre for Medium-Range Weather Forecasts.

Author Contributions M.J. and M.R. designed the study and are responsible for the integrity of the manuscript; M.J. performed the analysis and all calculations. M.J., M.R., P.C., S.I.S. and M.L.G. mainly wrote the manuscript. J.S., G.B., D. Gerten, J.H., J.K., Q.M., K.O., S.R., N.V., E.W., S.Z. and K.Z. contributed independent evapotranspiration model results. N.G. provided remotely sensed FAPAR data; R.d.J. and A.J.D. provided the TRMM soil-moisture data. E.T. and U.W. contributed to data processing. A.C., J.C., D. Gianelle, M.L.G., B.E.L., W.E., B.M., L.M., D.P., A.D.R., O.R. and C.W. contributed data provision or data processing. All authors discussed and commented on the manuscript.

Author Information Reprints and permissions information is available at www.nature.com/reprints. The authors declare no competing financial interests. Readers are welcome to comment on the online version of this article at www.nature.com/nature. Correspondence and requests for materials should be addressed to M.J. (mjung@bgc-jena.mpg.de) and M.R. (mreichstein@bgc-jena.mpg.de).